Eur. Phys. J. D **24**, 93–96 (2003)
DOI: 10.1140/epjd/e2003-00146-1

THE EUROPEAN PHYSICAL JOURNAL D

Magnetic properties of iron nitride-alumina nanocomposite materials prepared by high-energy ball milling

S.R. Mishra[1,a], G.J. Long[2], F. Grandjean[3], R.P. Hermann[3], S. Roy[4], N. Ali[4], and A. Viano[5]

[1] Department of Physics, University of Memphis, Memphis, TN 38152, USA
[2] Department of Chemistry, University of Missouri-Rolla, Rolla, MO 65409-0010, USA
[3] Department of Physics, University of Liège, 4000 Sart-Tilman, Belgium
[4] Department of Physics, Southern Illinois University, Carbondale, IL 62901-4401, USA
[5] Department of Physics, Rhodes College, Memphis, TN 38112-1690, USA

Received 10 September 2002
Published online 3 July 2003

Abstract. The structural and magnetic properties of the granular iron nitride-alumina composite materials, $(Fe_xN)_{0.2}(Al_2O_3)_{0.8}$ and $(Fe_xN)_{0.6}(Al_2O_3)_{0.4}$, fabricated using high-energy ball milling have been determined by using X-ray diffraction, Mössbauer spectroscopy, and magnetization measurements. The Mössbauer spectra, fit with a distribution of hyperfine fields between zero and 40 T, indicate that the weighted average field decreases with increasing milling time. The isomer shift increases with milling time because of a reduced iron 4*s*-electron density at the grain boundaries. Coercive fields as high as 325 and 110 Oe are obtained for $(Fe_xN)_{0.2}(Al_2O_3)_{0.8}$ at 5 and 300 K, respectively; the increase in the coercive field upon cooling indicates the presence of superparamagnetic particles. The coercive field increases with milling time because of the reduced particle size. The decrease in the magnetization results from the increase in both the superparamagnetic fraction and the concentration of surface defects with increased milling time.

PACS. 75.50.Tt Fine-particle systems; nanocrystalline materials – 81.20.Wk Machining, milling – 76.80.+y Mössbauer effect; other gamma-ray spectroscopy

1 Introduction

The sol-gel technique [1–3] has been widely used to disperse magnetic particles in an oxide matrix and a considerable enhancement in magnetic properties has been reported for such particles. Mechanical milling is an alternative technique that can produce a fine dispersion of magnetic particles in an oxide matrix [4]. The dispersion of iron particles in an alumina or silica matrix results in a considerable improvement in their magnetic properties [4–7], an improvement that is correlated with the reduction in particle size. However, as far as we can determine, there have been no previous studies of mechanically milled metal-metalloid-ceramic materials. The Fe_xN metal-metalloid is of importance to the magnetic recording industry because of its high saturation magnetization and coercivity [8] as compared to Fe_2O_3 [9], and its resistance to environmental damage [10]. More specifically, Fe_4N, has a saturation magnetization, σ_s, of 193 emu/g and a coercivity, H_c, of 1000 Oe, whereas Fe_2O_3 or cobalt modified iron oxide has a σ_s of 60−80 emu/g.

Mechanical alloying has been used to obtain supersaturated alloys, metastable phases, and amorphous materials, and to prepare new nanostructured materials [11]. Mechanical milling by its nature forces particles into close contact, thus often enhancing the interparticle magnetic interactions. Mechanical milling consists of repeated fracture, mixing, and cold welding of a fine blend of metal, oxide, and/or alloy particles resulting in size reduction [12] and sometimes in chemical reactions [13]. Indeed, an alloying or mechanochemical reaction can take place if the components of the mixture include metals and non-metals. In a metallic-ceramic mixture a displacement reaction can occur and, as a consequence, materials with enhanced magnetic properties may be obtained [14]. Often, competition between various components of the sample's magnetic anisotropy and its crystallinity obscures the true nature of the final magnetic state of the material. Thus, an accurate description of a mechanically milled magnetic material is often difficult and leads to unanswered questions such as why do mechanically milled particles of metals [15] and oxides [16] sometimes exhibit spin glass like behavior and sometimes spin disorder at the particle surface [17]?

The objective of this work is to investigate the structural and magnetic properties of an Fe_xN-alumina composite that consists of fine Fe_xN particles dispersed in an alumina matrix through mechanical ball milling.

[a] e-mail: srmishra@Memphis.edu

The structural and magnetic properties of the resulting composites have been investigated in order to determine the influence of milling on these properties.

2 Experimental methods

The starting materials consisted of 99.99% pure 325 mesh powders of Fe_xN and Al_2O_3. Approximately 10 g of the appropriate amounts of Fe_xN and Al_2O_3 were placed in a tungsten carbide vial with a sample to ball mass ratio of 1:20. The compositions studied herein are $(Fe_xN)_{0.2}(Al_2O_3)_{0.8}$ and $(Fe_xN)_{0.6}(Al_2O_3)_{0.4}$. The materials were milled for 4, 8, 16, 32, and 64 hours at 400 rpm in a Fritsch planetary ball mill in the presence of absolute ethanol in order to prevent oxidation.

X-ray diffraction patterns have been obtained with a Philips PC-APD3520 diffractometer and Cu K_α radiation. The particle sizes were determined with the Scherrer formula [18] after taking into account instrumental broadening. The dependence of the magnetic properties on the milling time has been investigated as a function of temperature on a SQUID magnetometer. Hyperfine parameters have been obtained from Mössbauer spectra measured on a constant-acceleration spectrometer which utilized a room-temperature rhodium matrix cobalt-57 source and was calibrated at room temperature with α-iron foil. The absorbers contained 30 mg/cm^2 of sample and the spectra have been fit with a 0 to 40 T distribution of hyperfine fields by using the method of Wivel and Mørup [19]. These fits use a distribution of 22 sextets, each of which has the same isomer shift, δ, referred to α-iron at room temperature, quadrupole shift, and linewidth; the components areas of each sextet were constrained to be in the ratio of 3:2:1:1:2:3. The quadrupole shifts are always essentially zero and the accuracy of the isomer shifts, quadrupole shifts, and linewidths is estimated to be ± 0.01 mm/s and the accuracy of the weighted average hyperfine fields is estimated to be ± 0.2 T.

3 Results and discussion

The X-ray diffraction pattern of the iron nitride starting material reveals that it is a mixture of Fe_3N and Fe_4N in the ratio 1:2; the patterns show no traces of any iron oxides, see Figure 1. The diffraction peaks observed for all the milled materials can be identified as either those of Fe_xN or Al_2O_3. Four hours of milling lead to a dramatic reduction in the intensity of the (111), (200), and (220) reflections of Fe_4N, and only one Fe_3N reflection, the (-1-11) reflection at $2\theta = 43.8°$, remains after eight hours of milling. The results clearly show a gradual decrease in peak intensities and an increase in their widths as a consequence of the particle size reduction and induced strain. However, both Fe_3N and Al_2O_3 remain crystalline after 64 hours of milling, a crystallinity which contrasts with the amorphous ceramic matrix observed in granular metal-ceramic films [6]. The particle diameter measured using the prominent peak of Fe_3N is shown in Figure 2a. Rapid grain size reduction occurs within the first 8 hours of milling; after 8 hours the grain size is less effectively reduced and a limiting diameter is approached. This behavior has been observed [20] earlier and results from the ability of the milled particles to withstand further deformation as they are work hardened by the milling process. The difference in particle diameters between the

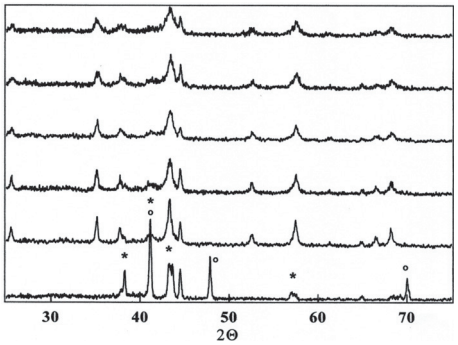

Fig. 1. The X-ray diffraction patterns of Fe_xN and $(Fe_xN)_{0.2}(Al_2O_3)_{0.8}$ obtained as a function of milling time. The milling time increases from 0 hours, bottom, to 4, 8, 16, 32, and 64 hours, top. The observed diffraction peaks may be identified as either those of Fe_3N, (*), γ'-Fe_4N, (○), or Al_2O_3.

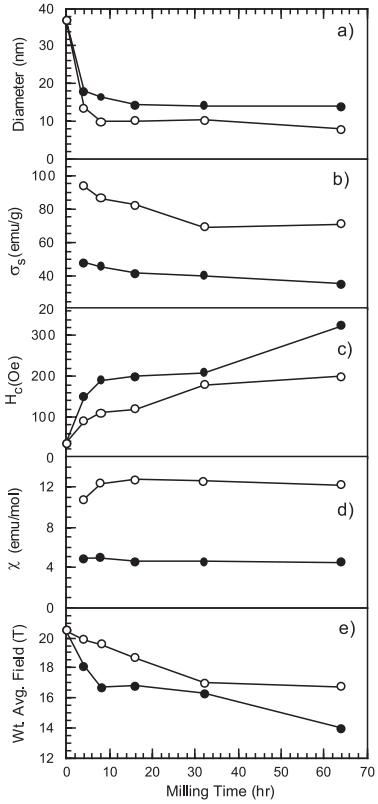

Fig. 2. The Fe_xN particle diameter (a), the 5 K and 5 T saturation magnetization, (b), the 5 K coercive field, (c), the 5 K molar magnetic susceptibility, (d), and the 295 K weighted average hyperfine field, (e), as a function of milling time for $(Fe_xN)_{0.2}(Al_2O_3)_{0.8}$, (●), and $(Fe_xN)_{0.6}(Al_2O_3)_{0.4}$, (○).

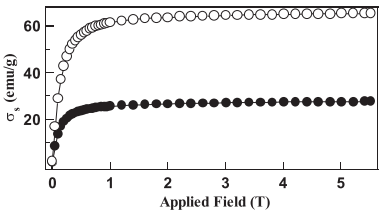

Fig. 3. The field dependence of the 300 K magnetization of $(Fe_xN)_{0.2}(Al_2O_3)_{0.8}$, (•), and $(Fe_xN)_{0.6}(Al_2O_3)_{0.4}$, (∘), obtained after milling for 64 hours.

$(Fe_xN)_{0.2}(Al_2O_3)_{0.8}$ and $(Fe_xN)_{0.6}(Al_2O_3)_{0.4}$ composites is evident from the width of the X-ray diffraction peak; the former has a larger Fe_3N grain diameter than the latter. This difference may be understood as follows. In $(Fe_xN)_{0.2}(Al_2O_3)_{0.8}$, the Fe_3N grains are more dispersed in the alumina matrix than in $(Fe_xN)_{0.6}(Al_2O_3)_{0.4}$ and, thus, they have a smaller probability of colliding during milling with the balls and the walls of the mill and, hence, they have a larger limiting grain diameter, but the basic behaviour upon milling is the same for both composite materials and in both cases the extent of amorphisation increases with milling time.

The coercivity and saturation magnetization of nanocomposite materials depend sensitively on particle size. The low 300 K saturation magnetizations of 28 and 62.5 emu/g observed for the 64 hour milled $(Fe_xN)_{0.2}(Al_2O_3)_{0.8}$ and $(Fe_xN)_{0.6}(Al_2O_3)_{0.4}$ nanocomposites, respectively, see Figure 3, as compared to the 295 K bulk saturation magnetization of 123 emu/g obtained for Fe_3N, are attributed both to the presence of surface defects and the presence of a superparamagnetic fraction [21,22] which is suggested by the lack of saturation even at 5 T. For both materials the magnetization measured at 5 K and 5 T decreases with milling time to a composition-dependent value as is shown in Figure 2b.

Coincident with the decrease in particle size, a distinct magnetic hardening process takes place upon milling. The coercive field, a measure of magnetic hardening, obtained at 5 K increases with milling time as is shown in Figure 2c. A comparison of Figures 2b and 2c indicates that the decrease in magnetization and the increase in coercive field result directly from the decrease in the Fe_3N particle diameter as is shown in Figure 2a. Even though the particle diameter is smaller for $(Fe_xN)_{0.6}(Al_2O_3)_{0.4}$, its coercive fields are smaller than those of $(Fe_xN)_{0.2}(Al_2O_3)_{0.8}$ most likely because of an increase in the magnetic interactions between the Fe_3N particles in the samples with a higher Fe_xN content. This explanation is supported by the observed increase in the molar susceptibility of $(Fe_xN)_{0.6}(Al_2O_3)_{0.4}$ with milling time, see Figure 2d. The increased susceptibility, which may result from crystalline aggregates with intercrystalline interactions, indicates a decrease in the magnetic anisotropy of these particles, particles which can then easily align with the applied field. In contrast, the magnetic susceptibility observed for $(Fe_xN)_{0.2}(Al_2O_3)_{0.8}$ is smaller and essentially remains constant with milling time because the non-interacting

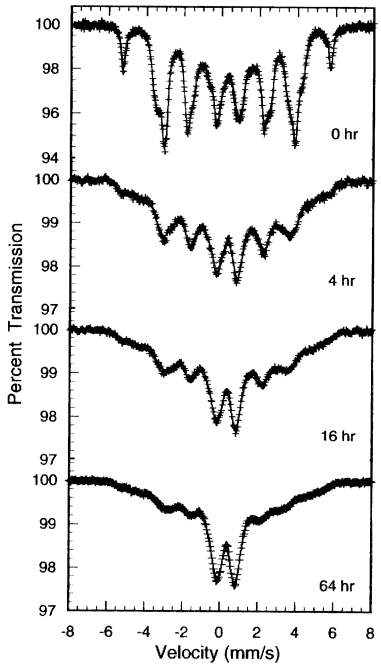

Fig. 4. The 295 K Mössbauer spectra of $(Fe_xN)_{0.2}(Al_2O_3)_{0.8}$ obtained after milling for the indicated times.

Fe_3N particles are more highly dispersed and have weaker magnetic interactions [4].

The 295 K Mössbauer spectra of $(Fe_xN)_{0.2}(Al_2O_3)_{0.8}$ obtained after milling are shown in Figure 4 and very similar spectra have been obtained for $(Fe_xN)_{0.6}(Al_2O_3)_{0.4}$. The Fe_xN spectrum is fit [19] with four sextets, three corresponding to Fe_4N and one corresponding to Fe_3N, and one broad central doublet assigned to the very fine superparamagnetic fraction present in the composite powder. The weighted average hyperfine fields of $(Fe_xN)_{0.2}(Al_2O_3)_{0.8}$ and $(Fe_xN)_{0.6}(Al_2O_3)_{0.4}$ decrease with milling time, see Figure 2e, as the Fe_xN particle size decreases and the amount of amorphous material increases. Both Figure 4 and a related temperature dependent study [23] of the Mössbauer spectra of these materials indicate that at higher temperatures they contain a significant fraction of a superparamagnetic iron phase, a fraction which increases with milling time. Because the superparamagnetic relaxation time is proportional to KV, the product of the magnetic anisotropy and the particle volume [24,25], the samples with longer milling times and thus smaller volumes, have shorter relaxation times. As a result a broadened superparamagnetic doublet appears in the 295 K Mössbauer spectra.

The 295 K isomer shift, δ, of non-milled Fe_xN is *ca.* 0.25 mm/s, which is the expected average isomer shift of a mixture containing Fe_4N, which has a δ of 0.20 mm/s, and Fe_3N, which has a δ of 0.28 mm/s [26]. After four hours of milling with Al_2O_3, δ increases to 0.30 mm/s, a value close to that of pure Fe_3N. Although the particle diameter of $(Fe_xN)_{0.6}(Al_2O_3)_{0.4}$ is smaller than that of $(Fe_xN)_{0.2}(Al_2O_3)_{0.8}$ its isomer shift is lower. The higher isomer shifts observed for $(Fe_xN)_{0.2}(Al_2O_3)_{0.8}$ as

compared with $(Fe_xN)_{0.6}(Al_2O_3)_{0.4}$ can be attributed to the lower s-electron density. This increase in isomer shift is believed to be due to the reduced s-electron density at the grain boundaries, the reduced particle sizes, and the strain in the crystal lattice [27,28].

4 Conclusions

This work was carried out to explore the prospect of producing ultrafine Fe_xN particles by ball milling Fe_xN with an insulating component, namely alumina. Structural studies show the rapid elimination of the iron rich Fe_4N phase as milling time increases. Because of the reported transformation of Fe_4N into Fe_3N at higher temperatures [29], it may be concluded that mechanical alloying provides enough activation energy for this transformation to occur. It has also been reported that iron particles dispersed in an insulating matrix show improved magnetic [30] and mechanical properties [31]. A reduction in the particle size of Fe_xN leads to a decrease in the saturation magnetization and a corresponding increase in the coercivity. The observed enhancement in coercivity for the Fe_xN particles likely results from a combination of particle size effect, surface defects, and mechanical stress. The presence of a superparamagnetic component in the Mössbauer spectra and the decrease in saturation magnetization are related to the particle size. Further study is needed to determine how these factors contribute to the coercivity. The observed increase in the isomer shift and rapid decrease in hyperfine field in the highly dispersed magnetic particles of $(Fe_xN)_{0.2}(Al_2O_3)_{0.8}$ are compatible with surface defects, defects which also require further investigation.

The authors thank the University of Memphis for its support during the course of this work. This work was supported in part by the "Fonds National de la Recherche Scientifique", Brussels, Belgium, grant 9.456595.

References

1. L.C. Klein, in *Nanomaterials: Synthesis, Properties and Applications*, edited by A.S. Edelstein, R.C. Cammarata (Institute of Physics Publishing, Bristol, PA, 1996)
2. V. Pilai, D.O. Shah, J. Magn. Magn. Mater. **163**, 243 (1996)
3. C.J. Brinker, G.W. Scherer, *Sol-Gel Science: The Physics and Chemistry of Sol-Gel Processing* (Academic Press, New York, 1990)
4. M. Paradvi-Hovarth, IEEE Trans. Magn. **28**, 3186 (1992)
5. A. Gavrin, C.L. Chien, J. Appl. Phys. **67**, 938 (1990)
6. C.L. Chien, in *Science and Technology of Nanostructured Magnetic Materials*, edited by G.C. Hadjipanayis, G.A. Prinz (Plenum Press, New York, 1991)
7. T. Ambrose, A. Gavrin, C.L. Chien, J. Magn. Magn. Mater. **116**, L311 (1992)
8. X. Bao, R.M. Metzger, W. Doyle, J. Appl. Phys. **73**, 6734 (1993)
9. K. Tagawa, E. Kita, A. Tasaki, Jpn J. Appl. Phys. **21**, 189 (1982)
10. T.-H.D. Lee, S. Hu, N. Madulid, IEEE Trans. Magn. **MAG-24**, 2880 (1987)
11. S.J. Campbell, H. Gleiter, in *Mössbauer Spectroscopy Applied to Magnetism and Materials Science*, edited by G.J. Long, F. Grandjean (Plenum Press, New York, 1996), p. 241
12. T. Kosmac, T.H. Courtney, J. Mater. Res. **7**, 1519 (1992)
13. C.C. Koch, Ann. Rev. Mater. Sci. **19**, 121 (1989)
14. J. Ding, W.F. Miao, E. Pirault, R. Street, P. McCormick, J. Alloys Compd. **267**, 267 (1998)
15. E. Bonetti, B.L. Del, D. Fiorani, D. Rinaldi, R. Caciuffo, A. Hernando, Phys. Rev. Lett. **83**, 2829 (1999)
16. R.H. Kodama, A.E. Berkowitz Jr, E.J. McNiff, S. Foner, Phys. Rev. Lett. **77**, 394 (1999)
17. D.V. Dimitrov, G.C. Hadjipanayis, V. Papaefthymiou, A. Simopoulos, J. Magn. Magn. Mater. **188**, 8 (1998)
18. B.D. Cullity, *Elements of X-ray Diffraction* (Addison Wesley, Reading, MA, 1978), p. 100
19. C. Wivel, S. Mørup, J. Phys. E: Sci. Instrum. **14**, 605 (1981)
20. J.S. Benjamin, Sci. Am. **234**, 40 (1976)
21. J. Bonger, A. Posinger, M. Reissner, W. Steiner, P. Mohn, K. Schwarz, S. Matar, G. Demazeau, J. Magn. Magn. Mater. **140-144**, 117 (1995)
22. N. Saegusa, A.H. Morrish, A. Tasaki, K. Tagawa, E. Kita, J. Magn. Magn. Mater. **35**, 123 (1983)
23. S.R. Mishra, G.J. Long, F. Grandjean, R.P. Hermann, S. Roy, A. Viano, N. Ali, in preparation
24. S. Mørup, J.A. Dumesic, H. Tpsøe, in *Applications of Mössbauer Spectroscopy*, edited by R.L. Cohen (Academic Press, New York, 1980), p. 1
25. A. Aharoni, Phys. Rev. **135**, A447 (1964)
26. P. Schaaf, Hyperf. Interact. **111**, 113 (1998)
27. V.K. Sankaranarayan, N.S. Gajbhiye, J. Am. Ceramic Soc. **73**, 1301 (1990)
28. H. Ouyang, B. Fultz, H. Kuwano, in *Nanophase and Nanocrystalline Structures*, edited by R.D. Shull, J.M. Sanchez (TMS, Pennsylvania, 1992)
29. R.N. Panda, N.S. Gajbhiye, IEEE Trans. Magn. **MAG-34**, 542 (1998)
30. A.K. Giri, C. De Julian, J.M. Gonzalez, J. Appl. Phys. **76**, 6573 (1994)
31. T.E. Schlesinger, R.C. Cammarata, A. Gavrin, C.L. Chien, M.F. Ferber, C. Hayzelden, J. Appl. Phys. **70**, 3275 (1991)